Exploring Deformation Mechanisms in Nanostructured Materials

JULIA R. GREER,[1,3] DONGCHAN JANG,[1] and X. WENDY GU[2]

1.—Division of Engineering and Applied Sciences, California Institute of Technology (Caltech), Pasadena, CA, United States. 2.—Division of Chemistry and Chemical Engineering, California Institute of Technology (Caltech), Pasadena, CA, United States. 3.—e-mail: jrgreer@caltech.edu

Useful properties of structural materials generally depend on their bulk microstructure. For centuries, improvements in structural materials relied heavily on processing, which in turn determined the resulting microstructure and properties. Materials sciences are entering an era in which specific properties of a material are obtained not only from its processing but also by controlling of the architecture of its constituents, often with sub-micron dimensions. To utilize this newly achievable nanoscale engineering precision in structural applications, it is imperative to quantify the deformation processes at each relevant scale, with special attention focusing on the importance of internal and external heterogeneities, for example grain boundaries, bi-material interfaces, phase boundaries, etc., on mechanical loading. It has been shown for single crystals that yield (and fracture) strengths increase with power-law dependence on sample size reduction when the micron scale is reached, and therefore, can no longer be inferred from bulk response or from the literature. Although these studies provide a powerful foundation for fundamental deformation processes operating at small scales, they are far from representing real materials used in structural applications, whose microstructure is often complex, containing boundaries and interfaces. Both homogeneous (i.e. grain and twin boundaries) and heterogeneous (i.e. phase and precipitate–matrix boundaries) interfaces in size-limited features are crucial aspects of the structural reliability of most modern materials. They are also of particular importance to damage initiation. This article provides a comprehensive overview of the state-of-the-art experimental and computational methods used to investigate mechanical behavior and microstructural evolution in small-scale metallic systems, deformation of which depends on intricate interactions of defects with internal interfaces and with free surfaces. Attention is focused on the effects of multiple grain boundaries spanning the sample volume (nanocrystalline and polycrystalline metals). This overview sheds light on the relative importance of intrinsic versus extrinsic length scale limitations on deformation mechanisms in nanostructured metals, which has significant implications for the development of new materials with tunable mechanical properties.

INTRODUCTION

A surprising increase in the tensile strength of single-crystalline metallic whiskers with decreasing diameter was first reported almost a century ago in the pioneering work of Taylor in 1924[1]; this was re-visited and confirmed some 30 years later by Brenner.[2,3] Their research sent a clear message that the mechanical properties of metals strongly depend on their microstructure, and on the size of the tested sample. In the last decade, there has been a revival of experimental investigations on the mechanical behavior of metals, especially at small scales—where not only the internal sample dimensions, i.e. grain size and inter-particle spacing, but also the external dimensions, i.e. diameter and length, are at the nanometer or micron level. Such a combination of limited external and internal characteristic length scales contributes to the overall mechanical response of the material, although the

individual contribution of each mechanism remains unclear.

In macroscopic samples, a material's stress–strain response (e.g., of polycrystalline metals) can be linked uniquely to the material's microstructure. Here, the characteristic property-governing scale is of the order of the grain structure. Since the seminal work of Hall[4] and Petch[5] in the 1950s, experimental evidence has confirmed a material-induced *intrinsic size effect*: a square root-type dependence of yield strength on average grain diameter,[6,7] exhibiting: *smaller is stronger*. Bulk nano-crystalline metals[8] with grain sizes above ∼30 nm are, essentially, stronger than their larger-grained and single crystalline counterparts.[9–11] Over the last two decades, an inverse effect has been observed for grain sizes below ∼10–20 nm[12,13] which was explained by a change in the deformation mechanisms,[6,14] trading conventional intra-grain dislocation activity for inter-grainular mechanisms, for example grain boundary (GB) sliding, rotation, migration, and shear.[15]

As modern fabrication techniques enable resolution of exhibiting device components at unprecedentedly small scales, material applications arise in which the characteristic length scale of the material microstructure approaches the size of individual structural members. Recently, our team has developed an ultra-light metallic micro-truss with a combined high stiffness ($E \sim \rho^2$) and extremely low density (0.9 mg/cm^3).[16] These micro-trusses are examples of multi-scale-designed materials because the sample itself has the lateral dimensions of several inches; the unit cells, which populate the lattice, are on the order of millimeters; the individual truss members are 1–4 mm long with hollow tube diameters of hundreds of microns; and the wall thickness can be varied between tens of nanometers and several microns. These walls are comprised of nano-crystalline nickel (with some residual phosphorus from the processing route), whose average grain size is on the order of 10 nm. The images and schematics of this hierarchy at each relevant material scale within this "meta-material" are shown in Fig. 1. To understand and predict the

mechanical response of such structures during lifetime operation, it is critical to elucidate properties such as yield strength, fracture toughness, deformability, and stiffness at the appropriate material length scale with the structural response, which is dictated by the cellular architecture. Separating the structural deformation response—i.e. that of the lattice—from the material-induced one—i.e. arising from the material's microstructure—is necessary for creation of predictive modeling tools. For example, continuum models that include the size-dependent mechanical properties of nano-crystalline Ni–P have shown promise in describing and optimizing the hollow-tube lattice architecture.[17]

Such ultra-light yet stiff and strong materials are desirable for many applications, for example in insulation and damping layers, as battery electrodes, and as components in aircraft and spacecraft. With the advent of nano-scale fabrication and patterning techniques, we—as a society—have begun to contemplate material systems in which feature size is comparable with the characteristic material microstructure dimensions. As a consequence, structural and material effects are no longer independent; instead, new and entirely uninvestigated deformation mechanisms arise from their competition. The very high surface-to-volume ratios of nanostructures introduce a new competing length scale that leads to the strong size effects in larger structures, which contain nanometer-sized constituents.[18,19] As society moves toward using architecture to create new materials with previously unexplored properties, the critical length scales of individual structural members and of the material microstructure become comparable with one another. Leaps, not strides, need to be taken to understand the deformation mechanisms which affect such material systems at each relevant length scale in a truly across-the-scales fashion.

Our recent work on the deformation of individual truss members within a nanocrystalline Ni microtruss revealed clear examples of a material-induced size-dependent properties.[17] In that work, individual vertically oriented hollow Ni cylinders with 6.6 nm grains and sub-micron-sized wall thick-
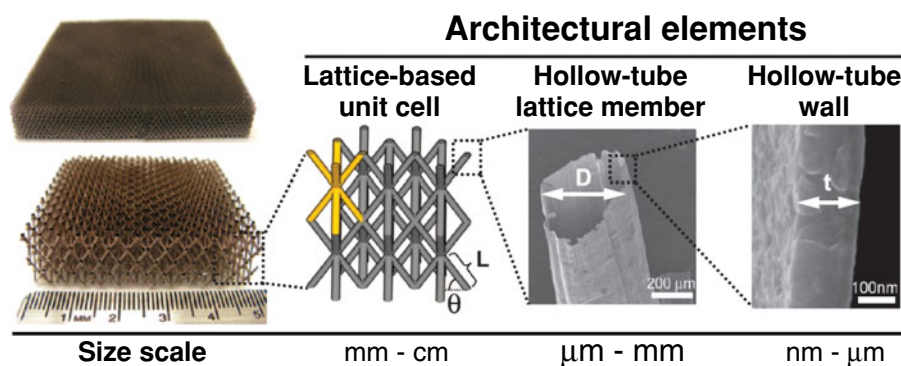

Architectural elements

Fig. 1. Cellular architecture and size scales in micro-lattices.[16]

nesses were subjected to severe in-situ uniaxial compression. These experiments revealed that their deformation was a strong function of both sample dimensions (i.e. wall thickness) and material microstructure (i.e. grain size and the presence of impurities). Distinct differences were observed between the collapse of the 500 nm-thick (i.e. "thick") and 150 nm-thick (i.e. "thin") nanocrystalline Ni cylinders, which were nominally identical except for the wall thickness. The thick samples collapsed in a brittle manner at 2% strain, via a single strain burst, whereas the thin samples underwent a gradual collapse, via a series of small discrete strain bursts, as shown in Figs. 2 and 3.[17] Further, the critical buckling stress of the thick samples was ~60 times higher than that of the thin samples, whose compressive strength was also 99.2% lower than that predicted by the shell buckling theory. The much lower compressive strengths observed for the thin samples were probably because of localized buckling and fracturing observed during the in-situ compression experiments, which did not occur in the thicker samples. These peculiar differences between the deformation of nominally identical hollow nanocrystalline Ni "shells", differing only in the wall thickness, cannot be explained by
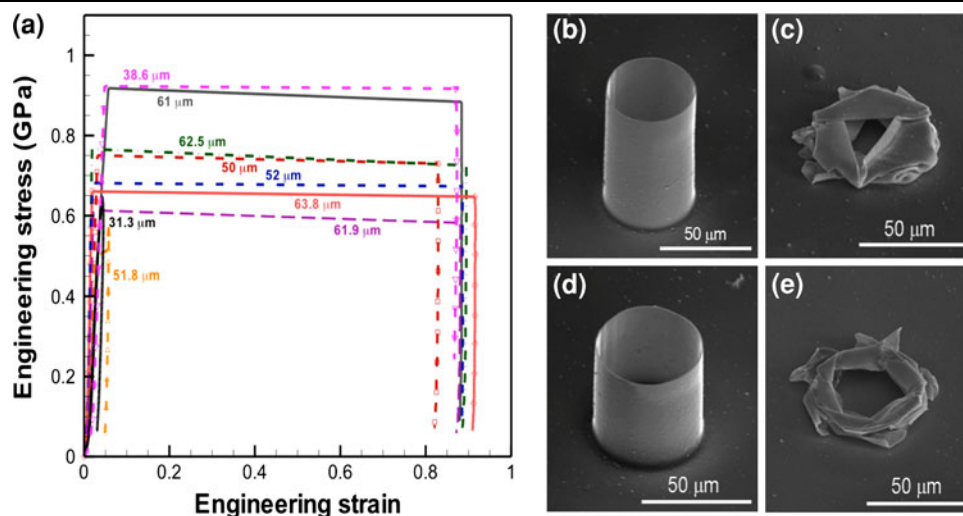

Fig. 2. Sudden collapse of 500 nm-thick hollow Ni cylinder under uniaxial compression with SEM images of before and after states and compressive stress–strain curves.[17]
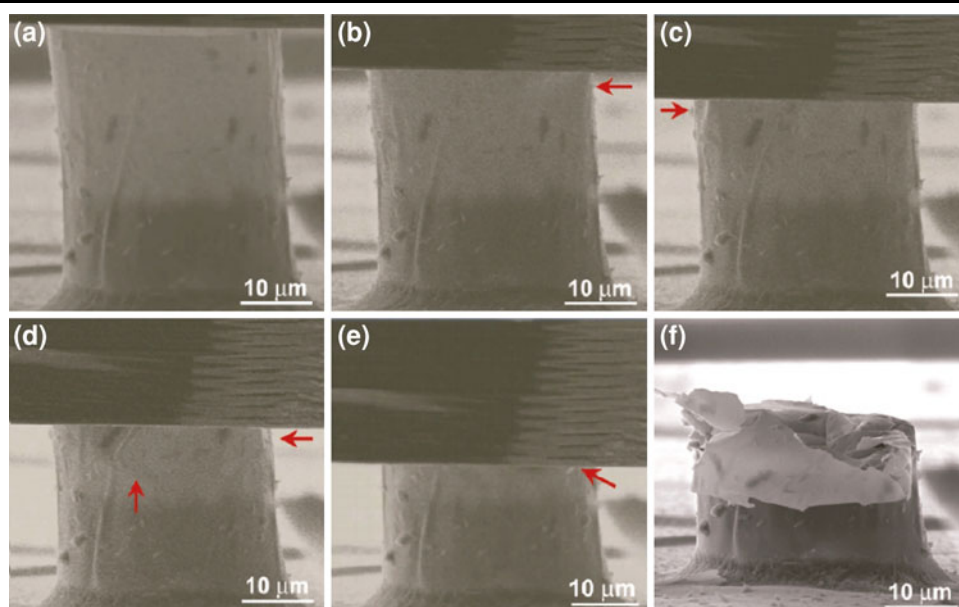

Fig. 3. Time progression during in-situ uniaxial compression of 150 nm-thick hollow Ni cylinder, which shows gradual deformability and localized fracture and folding.[17]

geometry effects alone. They were probably caused by the size-induced material mechanical behavior, specifically arising from the combination of the intrinsic and extrinsic material size effects.

BACKGROUND

To date, the material-induced and microstructure-induced size effects have been investigated independently, yet the combined effects of intrinsic and extrinsic dimensional limitations on materials' deformation behavior have not received as much attention.[19] In three-dimensionally designed materials, the combined effects of surfaces, internal interfaces (GBs), and crystal defects inside the parent solid collaboratively drive the overall hierarchical material's response. It is well-known that in nanocrystalline metals with sufficiently small grain sizes, intragrain dislocation activity gives way to intergrain mechanisms, for example GB sliding and rotation,[14] and stress-induced grain growth.[20] Single-crystalline metals, which contain no grain boundaries, have been widely shown to become stronger with size reduction.[19,21–25]

Size Effects in Single Crystals

Over the last decade, room-temperature uniaxial compression and tension experiments on a wide range of *single-crystalline* metallic micro and nanopillars have advanced our fundamental understanding of dislocation-based deformation processes at small scales.[19,21–28] The uniaxial compression methodology first introduced by Uchic et al.[22] was extended to the nano-scale by Greer and Nix[21] who fabricated single-crystalline Au nano-pillars with diameters below 1 μm by "top-down" focused ion beam (FIB) methodology and discovered unprecedented strengths, up to 50 times higher than in the bulk. Since then, numerous tests on cylindrical face-centered and body-centered-cubic metallic nano-pillars have demonstrated that, at micron and sub-micron scales, sample size dramatically affects crystalline strength, albeit differently for the different crystal symmetries.

Among others, Dou and Derby[30] summarized compressive-strength data for single-crystalline Au, Al, Ni, and Cu (all fcc metals) and reported the existence of a universal law of the form $\sigma_{res}/\mu = A(D/b)^m$ where μ is the shear modulus, σ_{res} is the shear stress resolved onto the $\langle 110 \rangle / \{111\}$ slip system, D is pillar diameter, and b is the Burgers vector magnitude. A seemingly universal slope for such size-induced strengthening in fcc metals, m, was determined to be close to -0.6.[19,23,30]

To date, uniaxial micro-deformation studies include but are not limited to the following fcc metals: Ni and Ni-based superalloys,[22,31–34] Au[21,35–38] Cu,[24,26,28,39–44] and Al;[45–47] bcc metals: Mo and alloys, Nb, Ta, W, and V,[48–53] hcp metals: Mg and Ti,[54–58] tetragonal low-temperature metals: In, Sn, and Pb,[59] Gum metal,[60] nanocrystalline metals,[61,62] shape

memory alloys,[63–69] and a variety of metallic glasses.[70–73] Most of these experiments revealed a strong dependence of flow strength on sample diameter, because of the activation of unique, defect-driven deformation mechanisms in nano-scale plasticity, often characterized by stochastic stress–strain curves and size-dependent strengths (Fig. 4).

Intriguingly, in contrast with Taylor hardening, the flow strengths of these small structures seem to increase with reduction in the mobile-dislocation density. It turns out that the size effect is an intricate function of the initial material microstructure (i.e. dislocation density),[74–79] strain rate, temperature,[80,81] and experimental setup,[24,27] in addition to sample size. Some of the mechanisms responsible for this elevation in strength with reduced dimensions include dislocation starvation, which has been shown to occur in very small, i.e. smaller than ~125 nm diameter, nano-pillars deformed at sufficiently slow strain rates,[21,32,35,45,80] source truncation and subsequent exhaustion,[74,77,82–85] and percolation-based weakest-link theories.[45,74,84,86,87] Some of these models also capture the experimentally observed stochastic signature and reveal marginal[45,74,88] or no dislocation storage.[32,35,44]

Although the focus of this article is on the combined effects of nanometer-sized internal and external material dimensions, it is worth mentioning that our research group has extensively studied plasticity in nano-sized single crystals, with some recent work focusing on tension and compression of Cu and Fe nano-pillars with diameters between 50 nm and 500 nm.[34,43,44,89–94] These samples were fabricated by e-beam lithography and electroplating to avoid the adverse effects of Ga$^+$-ion damage, which is inevitable in traditional FIB-based fabrication.[43,75,90,95–99] Results revealed an identical size effect as the ubiquitously observed power-law for FIB-fabricated fcc nano-pillars with an exponent of ~-0.63, which demonstrated that it is the initial microstructure, i.e. the initial number and arrangement of dislocations and their sources, rather than fabrication methods that drives and defines the size effect. The results of this research also demonstrated that at the nano-scale not only do the sample dimensions and the initial microstructure of the sample matter, but the strength becomes highly sensitive to the quasi-static strain rate, which is highly uncharacteristic for macroscopic fcc metals.[91] This emergence of strain-rate sensitivity may serve as proof of thermal contribution to nanoplasticity, suggesting that at these very small scales surface nucleation of dislocations, a thermally driven process, may have a non-trivial effect, as was predicted theoretically.[81]

Size Effects in Nanocrystalline Metals and Combined Size Effects

When polycrystalline metals are strained, the mobile dislocations inside the grains tend to pile-up
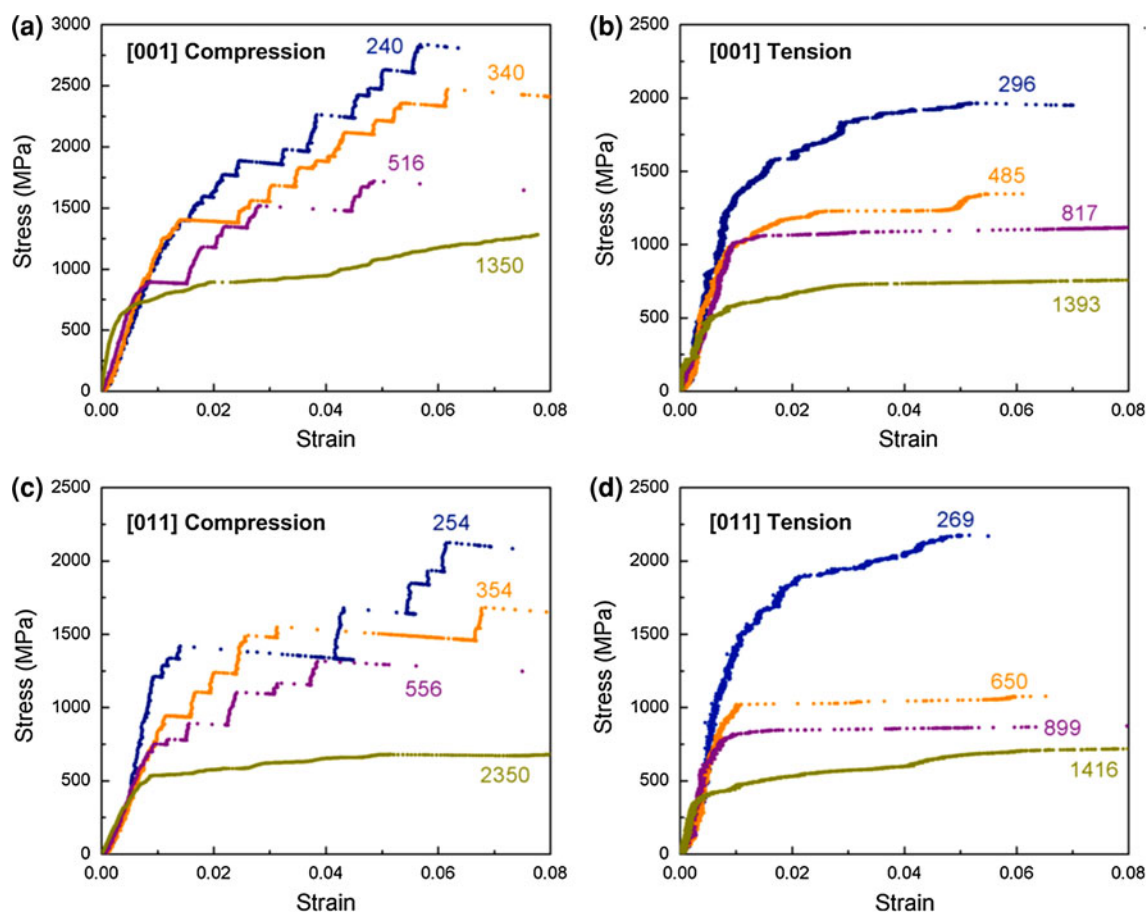
Fig. 4. Representative compressive and tensile stress–strain curves for single-crystalline Mo in two different orientations.[29] Numbers next to curves denote pillar diameters.

at grain boundaries (GBs), requiring the application of higher stresses to further propagate dislocations and plastically deform. In nanocrystalline metals, however, this Hall–Petch relationship[4,5] breaks down: materials become weaker at smaller grain sizes, a phenomenon often referred to as inverse Hall–Petch.[6,100] This grain-size-dependent transition in strengthening is shown schematically in Fig. 5. The specific deformation mechanisms responsible for the grain-size-dependent mechanical properties in nanocrystalline metals are still being debated, with some of the prominent proposed ones being grain rotation,[101–103] GB sliding,[104,105] partial dislocation emission and absorption at GBs,[106,107] diffusional creep,[107,108] and GB migration followed by grain growth.

The deviations from bulk-level mechanisms arise not only because of the small characteristic length scales but also because of surface proximity to the pertinent microstructural features. For example, molecular dynamics (MD) studies on polycrystalline nano-wires have reported strong GB–surface interactions and clear dependence of the stress–strain response on grain size and wire length-to-thickness ratio.[15]
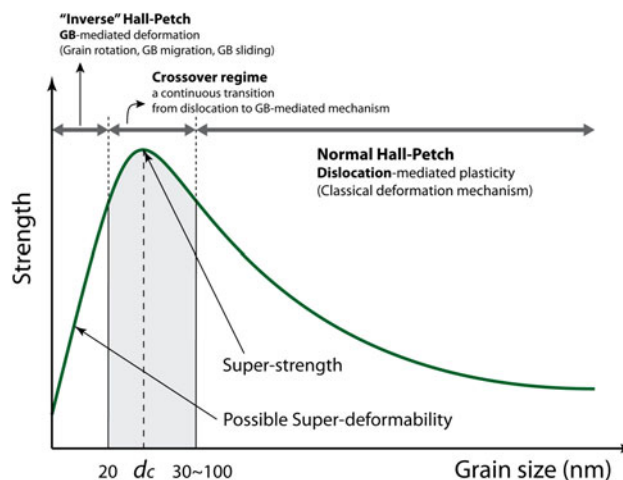

Fig. 5. Dependence of the strength of polycrystalline metals on grain size. For large grain sizes, strength is inversely proportional to grain size, i.e. smaller-grained metals are stronger (region labeled "Hall–Petch" on the plot). The strength of nanocrystalline metals, with grain sizes of ~20 nm and below, scales with grain size, i.e. smaller-grained metals are weaker (region labeled "inverse Hall–Petch" on the plot). The center region, in which strength is maximum, may occur for metals with grain sizes between 20 nm and 30 nm (illustration adapted from Ref. 19).
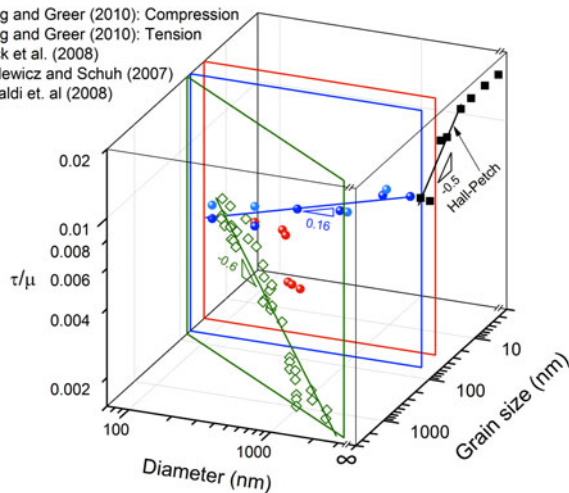
Fig. 6. Normalized stress as a function of both grain size, *d*, and pillar diameter, *D* (from Ref. 19).

These computations revealed that the weak GB–surface junctions formed preferential sites for nano-crack initiation, which accommodated large strains.[109] Although most computational studies so far have been limited to unrealistically small sample sizes and extremely high deformation rates, they have been useful in elucidating some of the atomic-level detail affecting mechanisms of nano-scale plasticity. Experimentally, Yang et al.[110] showed that the yield stress in polycrystalline copper micro wires was a strong function of the wire diameter-to-grain size ratio, and Jang et al.[19] demonstrated that nanocrystalline Ni nano-pillars had the "smaller is weaker" trend at pillar diameter-to-grain size ratios below ∼10.

Accurately modeling the deformation of nano-sized structural members is challenging because:

1 the limitations in size and viable strain rates render traditional MD simulations limiting;[111] and
2 sample dimensions of only several tens of nano-meters are well outside the realm of the continuum hypothesis of engineering models.

Well-known nano-scale deformation mechanisms, for example the formation of atom-thick chains in nano-wires,[15] nano-crystalline GB sliding followed by intergranular, surface-assisted fracture,[109] and the relaxation-and-recrystallization mechanism observed in Pt wires,[100] provide evidence that the existing atomistic models must be able to incorporate the mechanical response of nano-materials with a particular characteristic length scale and microstructure. Computational studies have provided essential details and uncovered physically relevant nano-scale deformation mechanisms. Although continuum and discrete dislocation models have efficiently described size effects in metals on the macroscale, they have failed to accurately

capture nano-scale deformation, in which the discrete nature of the crystal dominates and the continuum hypothesis breaks down. Nano-scale mechanical problems have been addressed mainly by MD,[112–118] which has provided indispensable insight into deformation mechanisms, energetics, and defect structures. For example, an early MD simulation on single-crystalline nano-sized Ni samples subjected to shear revealed size-dependence of yield stress on specimen dimensions.[119] A characteristic size scale based on the sample volume-to-surface-area ratio was postulated, which compared favorably with the experimental yield-stress data from indentation and torsion. MD simulations of Au nano-wires under tension at different strain rates and for different wire sizes at room temperature revealed yield strengths that increased with decreasing wire cross-sectional area.[120] MD simulations of nano-grained metals also helped understand the microstructural deformation mechanisms:[14] intergrain dislocation activity was replaced by intragrain mechanisms of, e.g., GB sliding and shear; grain interiors contained mainly partial dislocations. Because of size limitations, many MD simulations have focused on metal nano-wires[15,93,100,120–122] and have reported such characteristic nano-scale mechanisms as the formation of atom-thick chains prior to fracture,[15] or the atomic reconstruction–relaxation–recrystallization mechanism giving rise to zig-zag stress–strain behavior and abrupt slip localization on (111) planes in Pt[100] at low strain rates. Alternatively, nano-scale mechanics have been studied by Monte-Carlo methods; for example, simulations on single crystals under uniaxial compression using the Lennard–Jones potential in 2D confirmed a clear size effect with smaller samples yielding at higher stresses.[123]

IN-SITU STRAINING OF NANOCRYSTAL-LINE NI ALLOY NANOSTRUCTURES

Few experimental and computational studies have focused on the combined effects of polycrystalline or nanocrystalline microstructure and small sample size.[61,70,110,124] So far, the sought three-dimensional strength space of stress versus *D* (external diameter) and *d* (grain size) is sparsely populated, as shown in the recently summarized plot in Fig. 6 from Ref. 19. Earlier research in our group focused on uniaxial tension and compression experiments on nanocrystalline Ni-4%W nano-pillars whose average grain size was held constant at 60 nm while sample dimensions were reduced from 1.6 μm (∼42 grains across) to 100 nm (∼1.5 grains across).[62] These investigations revealed that the strength of the nanocrystalline nickel decreased by more than 30% as the pillar diameter was reduced to 100 nm—from 1.47 GPa to 0.86 GPa for compression and from 1.52 GPa to 0.98 GPa for tension. Global and local size-dependent weakening was observed, as manifested by both the lower yield

stresses in smaller pillars and by the presence of multiple undulations in the individual stress–strain curves. Both compressive and tensile stress–strain curves were not monotonic but composed of multiple cycles of nearly elastic loading followed by convex softening segments. The in-situ tests revealed that these undulations correspond to the formation of shear offsets, and in the cases when these offsets formed along a single plane, an entire sample-spanning shear band propagated across the cylinder. This deviation from the monotonic convex response, and failure, were found to commence at higher strains for larger nano-pillars than for smaller ones. Unlike the metallic single crystals, this was a demonstration of a "smaller is weaker" trend in small-scale samples, whose external and internal dimensions were concurrently reduced to micron and sub-micron scales. These findings are summarized in Fig. 7.

The origin of this "smaller is weaker" trend, and of the non-convex stress-signature, are particularly intriguing because the same 60-nm-grained Ni–W alloy with macroscopic dimensions has been reported to deform via dislocation-driven plasticity, as would be expected.[125,126] Yet the transmission electron microscopic (TEM) analysis of the same

material, but carved down to 100 nm-diameter and compressed, demonstrated that grain rotation, GB migration, and mechanical twinning took place as a result of deformation. Observing these phenomena in a nanocrystalline metal with grain sizes within the traditional Hall–Petch region ($d = 60$ nm) was surprising, especially because grain rotation and GB migration in the same-composition metals were previously observed only for grain sizes below 20 nm.[125,126] Our observations of grain shape alterations and grain boundary rotation in 100-nm samples after straining—in concert with a nearly 30% reduction in strength—suggested that relaxing the outer grains' constraints by introducing the free surfaces may have facilitated a transition in the deformation mechanism.

Samples with sufficiently large D/d ratios deformed via dislocation-driven plasticity, while grain-boundary activity was probably carrying the plastic strain in the smallest pillars, which had a so-called "bamboo" structure, i.e. containing no more than a single full grain across the diameter, making each grain a surface grain. The requirement of having a minimum number of grains within the sample to activate plasticity via dislocation pile-up against the grain boundaries, which leads to the
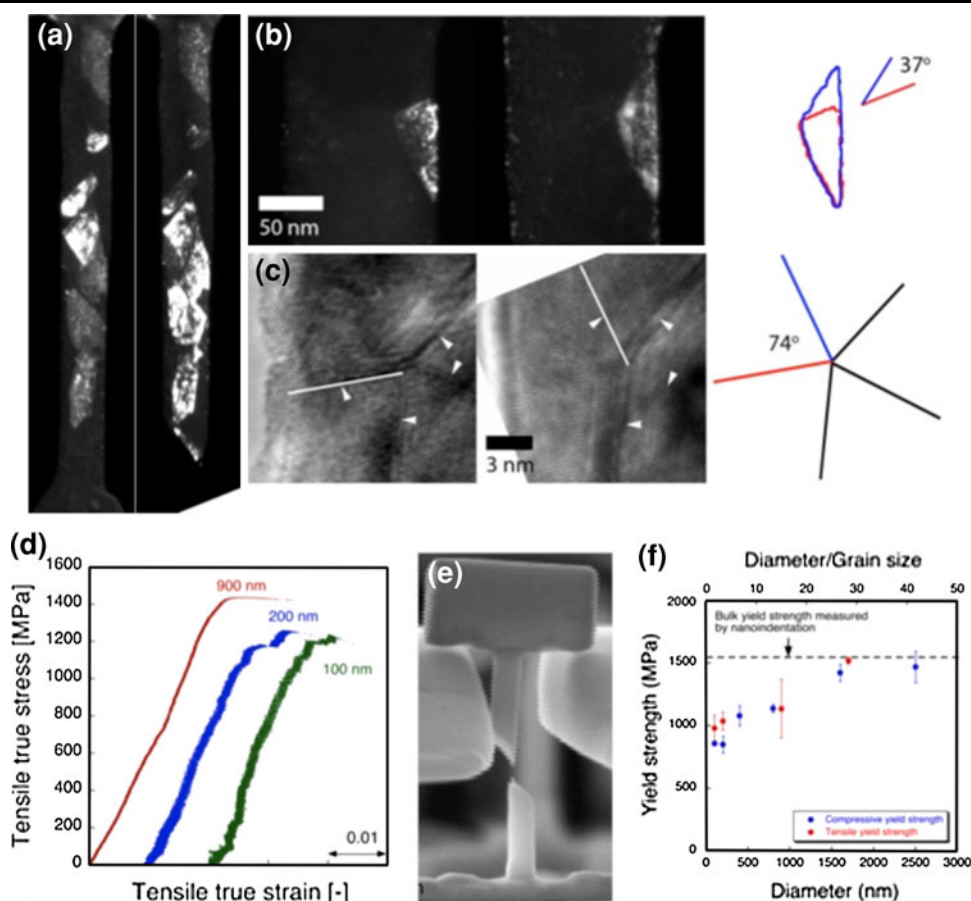

Fig. 7. Overall summary for nanocrystalline Ni-4%W (from Ref. 62).

well-known Hall–Petch strengthening, was reported as early as the 1960s.[127,128] Hansen et al.[127] remarked that a size effect was observed in poly-crystalline Al for specimens with D/d ratios below ~15, which corresponds to less than 10% volume fraction of surface grains, i.e. for a fixed grain size, samples with diameters smaller than that were also weaker because of the effects of the surface grains. This and earlier reports attributed such a concomitant strength reduction with diameter to relaxation of constraint-driven strengthening.[128]

Modeling the "Smaller is Weaker" Size Effect in Nanocrystalline Ni–4%W Nano-sized Samples

The mechanical properties of and deformation mechanisms in nanocrystalline metals have been well characterized.[6,7,12,14,90,105,125,129–135] Extensive investigations by Asaro et al. on modeling the deformation of nanocrystalline metals with macro-scopic dimensions suggest that plastic strain in 60 nm-grained Ni alloys deformed at the strain rates similar to the nano-pillar experiments in our work is carried by first the emission of perfect, as opposed to partial, dislocations from the grain boundaries and their subsequent glide.[136,137] In their model, the critical resolved shear stress, τ_c, required to produce and drive a full dislocation across a grain of size d, was formulated as: $\frac{\tau_c}{\mu} = \frac{b}{d}$, where μ is the shear modulus and b is the magnitude of the Burgers vector.

In our work, nanocrystalline Ni samples were shaped into nano-mechanical testing speci-mens—nano-cylinders (or nano-pillars) for com-pression and nano-dog-bone shapes for tension. These geometries at the nanometer scale are char-acterized by the substantial surface-area-to-volume-ratios, with greater effect of the outer surface grains on the mechanical response and deformation of the smaller-diameter samples. Such surface-dominated structures relax the outer constraints on the surface grains, and the mobile dislocations within these grains probably experience a strong effect of the image force during deformation. Upon mechanical loading, once the critical resolved shear stress in any of the outer surface grains has been reached, the mobile dislocations within the grains start gliding from, presumably, an adjacent inner grain boundary toward the free surface in response to the image force, as indicated by the simulations in Ref. 138.

A simple two-dimensional depiction of this pro-cess is shown in Fig. 8, which schematically outlines an edge dislocation positioned on a slip plane within a surface grain, as it glides from the grain boundary in the pillar interior toward the free surface in response to the image stress. To a first approxima-tion, this image stress may be represented as:

$$\tau_{\text{image}} = \frac{F}{b} = \frac{\mu b}{4\pi(1-v)d} \quad (1)$$

Here, F is the attractive image force per disloca-tion unit length, and v is Poisson's ratio. When dislocation glide is not impeded by obstacles such as impurities, point defects, or other dislocations, the shear stress required to emit and drive a dislocation across the surface grain is:

$$\tau_c = \frac{\mu b}{d} - \frac{\mu b}{4\pi(1-v)d} \quad (2)$$
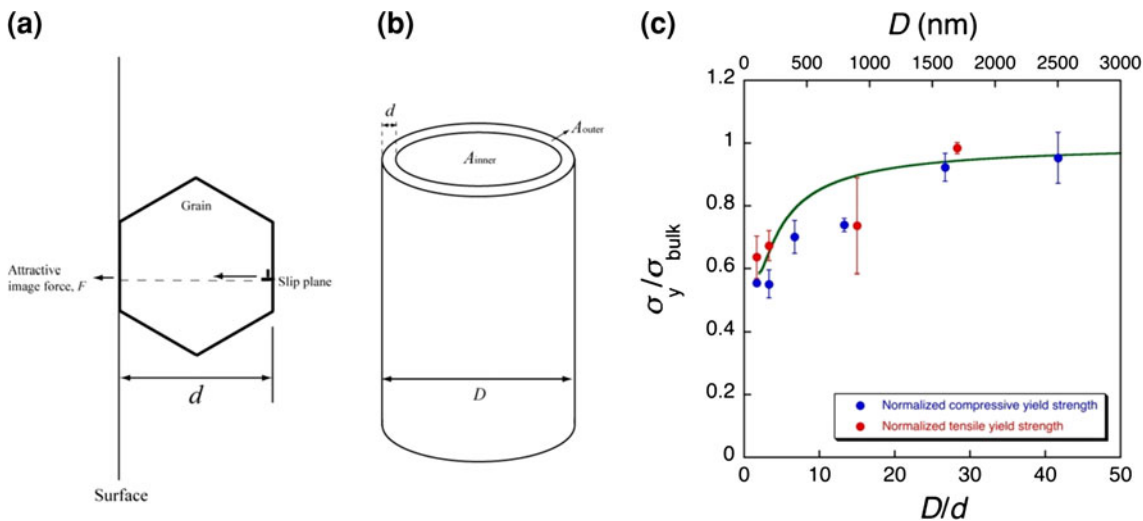

Fig. 8. (**a**) Schematic diagram showing dislocation emission and glide path, and the direction of the image force in a surface grain. (**b**) Schematic diagram showing the configuration of an outer annulus and inner core, used in the model. (**c**) Modeling results of yield strength as a function of D/d and D (*points* represent experimental data from Ref. 62).

The additional contribution from the image force, which pulls the dislocations out of the crystal, probably modifies the strength of the outer grains as compared with the inner ones. It is reasonable, therefore, to represent the overall compressive strength of the nanocrystalline pillar as a combination of an outer-grained annulus and an inner-grained cylindrical core, as illustrated in Fig. 8. Following the approach of Meyers et al.[6] we represent the overall yield strength of the pillar, σ_y, as the weighted sum of its constituents:

$$\sigma_y = \frac{A_{\text{inner}}}{A_{\text{total}}} \sigma_{\text{inner}} + \frac{A_{\text{outer}}}{A_{\text{total}}} \sigma_{\text{outer}} \qquad (3)$$

$$\sigma_y = \frac{(D-2d)^2}{D^2} \sigma_{\text{inner}} + \frac{\left(D - 2(D-2d)^2\right)}{D^2} \sigma_{\text{outer}} \quad (4)$$

$$\sigma_y = \left(1 - 2\frac{d}{D}\right)^2 \sigma_{\text{inner}} + \left(1 - \left(1 - 2\frac{d}{D}\right)\right)^2 \sigma_{\text{outer}}, \qquad (5)$$

where D is the pillar diameter, A_{inner} and A_{outer} are the cross sectional areas of the inner core and the outer annulus, respectively, and their sum is the total cross-sectional area of the pillar, A_{total}. σ_{inner} and σ_{outer} are the yield strengths of the inner core and the outer annulus, respectively. These axial strengths can be related to the resolved shear stresses by multiplying by the appropriate Taylor factors $\hat{m}_{\text{outer}}$ and $\hat{m}_{\text{inner}}$, such that $\sigma_{\text{outer}} = \hat{m}_{\text{outer}} \tau_a$ and $\sigma_{\text{outer}} = \hat{m}_{\text{outer}} \tau_c$.[139] We argue that a distinction between the outer and inner Taylor factors must be made to account for the strain compatibility along the GBs assumption, which is reasonable for macroscale samples but is unlikely for the less constrained outer grains.[128] We estimate $\hat{m}_{\text{outer}}$ to be close to 2, as has been reported for bamboo-structured metals.[128]

It is likely that this factor is underestimated because the reduction in the outer constraint is more pronounced for bamboo structures than for the annulus, whose inside wall remains constrained by the matrix. The Taylor factor for the grains deeply inside the pillar, $\hat{m}_{\text{inner}}$ was taken to be $\sim$3, a typical value for face-centered cubic polycrystals.[139] Substituting physically relevant values for Ni into this model: $\mu = 76\,GPa$, $v \sim \frac{1}{3}$, and $b = 0.249$ nm, and using the value of σ_{inner} obtained experimentally for the bulk sample, from which the pillars were made, the model predicts lowering of the yield strength with D/d ratio, as shown in Fig. 8(c). This phenomenological model is simple and 2-dimensional, and therefore does not capture many of the physical phenomena that may be attributed to size-induced effects, or to intriguing deformation mechanisms. For example, it clearly overestimates the

yield strength for the samples between D/d $\sim$10 and 20. Also, the active slip planes would be inclined at an angle to the surface, as opposed to being oriented perpendicular, as modeled here. This type of a geometrical effect is expected to affect the absolute magnitude rather than the overall trend. Most likely, plasticity in the nanocrystalline metallic nano-samples is driven by a combination of dislocation-driven mechanisms and grain boundary activity; the model developed here only accounts for dislocation plasticity. Despite these limitations, this phenomenological framework incorporates the effect of the softer outer core on the overall strength by accounting for the effects of the image stress and of the reduced Taylor factor for nanocrystalline nanostructures, and seems to explain the weakening trend well.

We subsequently discovered that for smaller grain sizes of $\sim$10 nm in 50-nm-diameter nickel pillars, strength was similar to that of bulk nanocrystalline Ni at the same grain size.[140]

More recently, similarly to the study by Jang and Greer,[62] Yang et al.[110] also investigated the tensile response of multiple grain boundary-containing polycrystalline metallic wires via in-situ mechanical testing inside an electron microscope. These samples had micron-sized dimensions of both the grains and the wire geometry. These authors established that the strength of the polycrystalline Cu wires was a function of both the absolute grain size, d, and the number of grains across the diameter, D. A composite model was constructed in which the authors surmised that the lowering of the yield stress with decreasing D/d ratio in polycrystalline metals was related to differences in the resistance of dislocations piling up against the grain boundaries in the interior of the sample versus those adjacent to the surface.[110] This comprehensive study revealed that the yield stress was significantly affected by both the grain size d and the specimen thickness D when the number of grains across the diameter was less than 10. With the increasing number of grains across the diameter, the Hall–Petch constants were found to increase, resulting in higher yield stresses for thicker samples for a given grain size. The results of these experiments are consistent with the aforementioned early metallurgical studies[127,128] with the possible discrepancy of the D/d ratio being closer to 10 in the work of Yang et al. and to 15 in the Cu samples. This difference may or may not be significant, because the deviation from Hall–Petch type strengthening was found to be material and grain size-dependent. The weighted-average iso-strain model developed in the work of Yang, et al. is intended to capture the plastic response of the micro rather than nano-grained Cu samples, which means that plasticity was accommodated entirely by dislocation activity. This model predicts a similar "smaller is weaker" trend as a function of the sample diameter-to-grain size ratio, D/d, as for the nanocrystalline Ni nano-sized samples.

Our on-going work is focused on compressive and tensile deformation of nanocrystalline platinum nano-pillars and also reveals a transition from bulk-level strengths to substantially weaker ones for diameter-over-grain-size fractions of $D/d \sim 5$. These nanocrystalline Pt nanopillars have sub-micron diameters, D, and a single grain size of 12 nm, d, such that the number of grains across the pillar diameter is systematically varied from ~ 5 to 80. These results are being prepared in a separate manuscript, and so far we are discovering that the strength of the nanocrystalline Pt does not deviate significantly from the bulk yield strength down to D/d ratios of 8, and the pronounced weakening occurs only in the smallest samples with diameters of 60 nm. We postulate that this lack of a size effect arises because the deformation is initiated and carried out mainly at the grain boundaries rather than being controlled by the free surfaces.

Our preliminary MD simulations reveal that the deformation may be controlled by either grain boundary sliding or by dislocation–nucleation, or by a combination of these mechanisms. In the cases where the deformation is controlled by dislocation nucleation, we observe two important limits:

- in *single crystals* the dislocation nucleation from the free surface dominates (at larger diameters, the pre-existing dislocations can be important also); and
- in the *nanocrystalline* pillars with diameters of more than a few grains, the nucleation of dislocations occurs predominantly at the grain boundary triple junctions that serve as stress concentrations, which developed, in part, as a result of grain boundary sliding.

Comparison of the experimental results for Ni and Pt suggests that the transition from bulk-like to the "smaller is weaker" regime depends on *both* the grain size, d, and the ratio of pillar diameter to grain size, D/d, and on the particular metal. It is also interesting to note that when D/d is relatively small, the fluctuations in the number of grains across the diameter could also be important.

SUMMARY AND OUTLOOK

The variety of materials that are being investigated in the context of size-dependent mechanical properties, both in terms of external dimensions and internal microstructure, has increased substantially over the last decade. Advances in fabrication techniques and sophisticated modeling capabilities facilitate unprecedented material characterization and exploration of new processing routes. Such a combined approach, in which at least the length scales between the experiments and the computations are within each other's reach, result in a powerful physical understanding of the emergent nano-size induced phenomena for solids. Although all this progress is exciting, it is critical that the researchers in this field take special care when conducting these experiments and sample synthesis because the data are significantly affected by experimental artifacts, geometry, and purity, to list a few. The community has now shown that size-dependent material strengths in the small-scale structures emerge because of both intrinsic and extrinsic characteristic length scales. These size effects are not universal, with the clear distinction between the "smaller is stronger" effect for single crystals and the "smaller is weaker" trend for nanocrystalline nanosamples, shown here. The combined effects of reduced dimensions must be actively investigated, and the next task for us as a community is to populate three-dimensional space with material strength plotted on the vertical axes and both the microstructural length scale (i.e. grain size, twin boundary spacing, nanolaminates spacing, phase boundary spacing, dislocation density) and the external dimensions (i.e. pillar diameter, film thickness, etc.) on both of the horizontal axes. When such a full layout of size effects is created, the feature size will enable the creation of revolutionary new materials with realistic technological applications.

REFERENCES

1. G.F. Taylor, *Phys. Rev.* 23, 655 (1924).
2. S.S. Brenner, *J. Appl. Phys.* 27, 1484 (1956).
3. S.S. Brenner, *J. Appl. Phys.* 28, 1023 (1957).
4. E.O. Hall, *Proc. Phys. Soc. B* 64, 742 (1951).
5. N.J. Petch, *J. Iron Steel Inst.* 174, 25 (1953).
6. M. Meyers, A. Mishra, and D. Benson, *Prog. Mater. Sci.* 51, 427 (2006).
7. J. Eckert, J. Holzer, C. Krill, and W. Johnson, *Acta Mater.* 55, 3749 (2007).
8. H. Gleiter, *Acta Mater.* 48, 1 (2000).
9. G. Nieman, J. Weertman, and R. Siegel, *Scr. Metall. Mater.* 24, 145 (1990).
10. F. Ebrahimi, G. Bourne, M. Kelly, and T. Matthews, *Nanostruct. Mater.* 11, 343 (1999).
11. A. Karimpoor, U. Erb, K. Aust, and G. Palumbo, *Scripta Mater.* 49, 651 (2003).
12. T. Nieh, and J. Wadsworth, *Scr. Metall. Mater.* 25, 955 (1991).
13. J. Eckert, J. Holzer, C. Krill, and W. Johnson, *J. Mater. Res.* 7, 1751 (1992).
14. H. Van Swygenhoven, Z. Budrovich, P. Derlet, and A. Hasnaoui, *Processing and Properties of Structural Nanomaterials*, ed. L. Shaw, C. Suryanarayana, and R. Mishra (Chicago, 2003) pp. 3–10.

15. X. Li, W. Hu, S. Xiao, and W.-Q. Huang, *Physica E* 40, 3030 (2008).
16. T.A. Schaedler, A.J. Jacobsen, A. Torrents, A.E. Sorensen, J. Lian, J.R. Greer, L. Valdevit, and W.B. Carter, *Science* 334, 962 (2011).
17. J. Lian, D. Jang, L. Valdevit, T.A. Schaedler, A.J. Jacobsen, W.B. Carter, and J.R. Greer, *Nano Lett.* 11, 4118 (2011).
18. J. Munilla, M. Castro, and A. Carnicero, *Phys. Rev. B* 80, 024109 (2009).
19. J.R. Greer, J.T. De Hosson, and Th.M. Jeff, *Prog. Mater. Sci.* 56, 654 (2011). ISSN 00796425.
20. T.J. Rupert, D.S. Gianola, Y. Gan, and K.J. Hemker, *Science* 326, 1686 (2009) ISSN 1095-9203, http://www.ncbi.nlm.nih.gov/pubmed/20019286.
21. J.R. Greer, W.C. Oliver, and W.D. Nix, *Acta Mater.* 53, 1821 (2005).
22. M.D. Uchic, D. Dimiduk, J.N. Florando, and W.D. Nix, *Science* 305, 986 (2004).
23. O. Kraft, P. Gruber, R. Mönig , and D. Weygand, *Annu. Rev. Mater. Res.* 40, 293 (2010).
24. G. Dehm, *Prog. Mater. Sci.* 54, 664 (2009).
25. M.D. Uchic, P. Shade, and D. Dimiduk, *Annu. Rev. Mater. Res.* 39, 361 (2009).
26. D. Kiener, W. Grosinger, G. Dehm, and R. Pippan, *Acta Mater.* 56, 580 (2008).
27. D. Kiener, C. Motz, and G. Dehm, *Mater. Sci. Eng. A* 505, 79 (2009). ISSN 09215093. http://linkinghub.elsevier.com/retrieve/pii/S0921509309000124.
28. D. Kiener, and A.M. Minor, *Acta Mater.* 59, 1328 (2011). ISSN 13596454. http://linkinghub.elsevier.com/retrieve/pii/S1359645410007391.
29. J.-Y. Kim, D. Jang, and J.R. Greer, *Int. J. Plast.* (2011).
30. R. Dou, and B. Derby, *Scripta Mater.* 61, 524 (2009).
31. D. Dimiduk, M. Uchic, and T. Parthasarathy, *Acta Mater.* 53, 4065 (2005).
32. Z.W. Shan, J. Li, Y. Cheng, A.M. Minor, S.A. Syed Asif, O.L. Warren, and E. Ma, *Phys. Rev. B* 77, 1 (2008). ISSN 13596454.
33. C. Frick, B. Clark, S. Orso, A. Schneider, and E. Arzt, *Mater. Sci. Eng. A* 489, 319 (2008). ISSN 09215093. http://dx.doi.org/10.1016/j.msea.2007.12.038.
34. R. Maa L. Meza, B. Gan, S. Tin, and J.R. Greer, *Small* 8, 1869 (2012). ISSN 1613-6829. http://www.ncbi.nlm.nih.gov/pubmed/22454244.
35. J.R. Greer, and W.D. Nix, *Phys. Rev. B* 73, 1 (2006).
36. C.A. Volkert, and E.T. Lilleodden, *Phil. Mag.* 86, 5567 (2006).
37. A.S. Budiman, S.M. Han, J.R. Greer, N. Tamura, J. Patel, and W.D. Nix, *Acta Mater.* 56, 602 (2008).
38. S.-W. Lee, S. M. Han, and W.D. Nix, *Acta Mater.* 57: 4404 (2009). ISSN 13596454. http://linkinghub.elsevier.com/retrieve/pii/S1359645409003401.
39. D. Kiener, C. Motz, T. Schoberl, M. Jenko, and G. Dehm, *Adv. Eng. Mater.* 8, 1119 (2006).
40. D. Kiener, W. Grosinger, and G. Dehm, *Scripta Mater.* 60, 148 (2009). http://linkinghub.elsevier.com/retrieve/pii/S1359646208006933.
41. D. Kiener, C. Motz, and G. Dehm, *Mater. Sci. Eng. A* 505, 79 (2009). ISSN 13596462.
42. R. Maass, S. Van Petegem, D. Grolimund, H. Van Swygenhoven, D. Kiener, and G. Dehm, *Appl. Phys. Lett.* 92 (2008).
43. A. Jennings, M. Burek, and J. Greer, *Phys. Rev. Lett.* 135503 (2010).
44. A.T. Jennings, and J.R. Greer, *Phil. Mag.* 91, 1 (2010).
45. K. Ng, and A.H.W., Ngan, *Scripta Mater.* 59, 796 (2008).
46. A. Kunz, S. Pathak, and J.R. Greer, *Acta Mater.* 59, 4416 (2011).
47. K.S. Ng, and A.H.W. Ngan, *Phil. Mag.* 89, 3013 (2009).
48. J.-Y. Kim, D. Jang, and J. R. Greer, *Scripta Mater.* 61, 300 (2009). ISSN 13596462.
49. J.-Y. Kim, and J.R. Greer, *Acta Mater.* 57, 5245 (2009).
50. A.S. Schneider, B.G. Clark, C.P. Frick, P. Gruber, and E. Arzt, *Mater. Sci. Eng. A* 508, 241 (2009).
51. H. Bei, S. Shim, E. George, M. Miller, E. Herbert, and G. Pharr, *Scripta Mater.* 57, 397 (2007).
52. H. Bei, Y. Gao, S. Shim, E. George, and G. Pharr, *Phys. Rev. B* 77, 2 (2008).
53. H. Bei, E. George, and G. Pharr, *Mater. Sci. Eng. A* 483–484, 218 (2008).
54. E. Lilleodden, *Scripta Mater.* 62, 532 (2010).
55. C.M. Byer, B. Li, B. Cao, and K. Ramesh, *Scripta Mater.* 62, 536 (2010).
56. J. Ye, R.K. Mishra, A.R. Pelton, and A.M. Minor, *Acta Mater.* 58 (2010).
57. Q. Yu, Z.-W. Shan, J. Li, X. Huang, L. Xiao, J. Sun, and E. Ma, *Nature* 463, 335 (2010).
58. Q. Sun, Q. Guo, X. Yao, L. Xiao, J.R. Greer, and J. Sun, *Scripta Mater.* (2011).
59. S.-W. Lee, and W.D. Nix, *Mater. Sci. Eng. A* 527, 1903 (2010).
60. E.A. Withey, A.M. Minor, D.C. Chrzan, J.W. Morris Jr., and S.Kuramoto, *Acta Mater.* 58, 2652 (2010).
61. A. Rinaldi, P. Peralta, C. Friesen, and K Sieradzki, *Acta Mater.* 56, 511 (2008).
62. D. Jang, and J.R. Greer, *Scripta Mater.* 64, 77 (2011).
63. B.G. Clark, D.S. Gianola, O. Kraft, and C.P. Frick, *Adv. Eng. Mater.* 12, 808 (2010).
64. C.P. Frick, S. Orso, and E. Arzt, *Acta Mater.* 55, 3845 (2007).
65. C.P. Frick, B.G. Clark, S. Orso, P. Sonnweber-Ribic, and E. Arzt, *Scripta Mater.* 59, 7 (2008).
66. C.P. Frick, B. Clark, S. Orso, A. Schneider, and E. Arzt, *Mater. Sci. Eng. A* 489, 319 (2008).
67. C.P. Frick, B.G. Clark, A.S. Schneider, R. Maaß, S. Van Petegem, and H. Van Swygenhoven, *Scripta Mater.* 62, 492 (2010).
68. J. San Juan, M.L. Nó, and C. Schuh, *Adv. Mat.* 20, 272 (2008).
69. J.M. San Juan, M.L. Nó, and C. Schuh, *Nat Nanotechnol.* 4 (2009).
70. D. Jang, and J.R. Greer, *Nat. Mater.* 9, 215 (2010).
71. D. Jang, C.T. Gross, and J.R. Greer, *Int. J. Plast.* 27, 858 (2010).
72. C.A. Volkert, A. Donohue, F. Spaepen, *J. Appl. Phys.* 103, 83539 (2008).
73. C. Chen, Y.T. Pei, J.T. De Hosson, *Phil. Mag. Lett.* 89, 633 (2009).
74. D. Norfleet, D. Dimiduk, S. Polasik, M. Uchic, and M. Mills, *Acta Mater.* 56, 2988 (2008).
75. S. Shim, H. Bei, M. Miller, G. Pharr, and E. George, *Acta Mater.* 57, 503 (2009). ISSN 13596454. http://linkinghub.elsevier.com/retrieve/pii/S1359645408006940.
76. K.E. Johanns, A. Sedlmayr, P. Sudharshan Phani, R. Mönig, O. Kraft, E.P. George, G.M. Pharr, *J. Mater. Res.* 27, 508 (2012). ISSN 2044-5326. http://journals.cambridge.org/abstract_S0884291411002986.
77. M. Legros, D. S. Gianola, and C. Motz, *MRS Bull.* 35 (2010).
78. F. Mompiou, and M. Legros, *Adv. Eng. Mater.* (2012). ISSN 14381656. http://doi.wiley.com/10.1002/adem.201200020.
79. F. Mompiou, M. Legros, A. Sedlmayr, D.S. Gianola, D. Caillard, and O. Kraft, *Acta Mater.* 60, 977 (2012). ISSN 13596454. http://linkinghub.elsevier.com/retrieve/pii/S1359645411007919.
80. A. Jennings, J. Li, and J. Greer, *Acta Mater.* 59, 5627 (2011).
81. T. Zhu, J. Li, A. Samanta, A. Leach, and K. Gall, *Phys. Rev. Lett.* 100, 1 (2008).
82. S.I. Rao, D. Dimiduk, T. Parthasarathy, M. Uchic, M. Tang, and C. Woodward, *Acta Mater.* 56, 3245 (2008).
83. T. Parthasarathy, S.I. Rao, D. Dimiduk, M. Uchic, D. Trinkle, *Scripta Mater.* 56, 313 (2007).
84. S.I. Rao, D. Dimiduk, M. Tang, T.A. Parthasarathy, M.D. Uchic, and C. Woodward, *Phil. Mag.* 87, 4777 (2007).
85. S. Oh, M. Legros, D. Kiener, and G. Dehm, *Nat. Mater.* 8 (2009).
86. S.I. Rao, M.D. Uchic, P.A. Shade, C. Woodward, and T.A. Parthasarathy, *Modell. Simul. Mater. Sci. Eng.* 20, 065001 (2012).

87. H.W. Ngan, and K.S. Ng, *Phil. Mag.* 90, 1937 (2010), ISSN 1478-6435, http://www.informaworld.com/openurl?genre=article&doi=10.1080/14786430903571487&magic=crossref||D404A21C5BB053405B1A640AFFD44AE3.

88. D. Dimiduk, C. Woodward, R. Lesar, and M.D. Uchic, *Science* 312, 1188 (2006).

89. J.R. Greer, J.-Y. Kim, and M.J. Burek, *J. Mater.* 61, 19 (2009).

90. M.J. Burek, J.R. Greer, *Nano Lett.* 10: 69 (2010). ISSN 1530-6992. http://www.ncbi.nlm.nih.gov/pubmed/19961184.

91. A. Jennings, and J. Greer, *J. Mater. Res.* 26, 2803 (2011).

92. A.T. Jennings, and J.R. Greer, *J. Mater. Res.* 26, 2803 (2011). ISSN 0884-2914. http://www.journals.cambridge.org/abstract_S0884291411003384.

93. C. Weinberger, A. Jennings, K. Kang, and J. Greer, *J. Mech. Phys. Solids* 60, 84 (2012).

94. A.T. Jennings, C. Gross, F. Greer, Z.H. Aitken, S.-W. Lee, C. Weinberger, and J. Greer, *Acta Mater.* 60, 3444 (2012).

95. H. Bei, S. Shim, M. K. Miller, G. Pharr, and E. George, *Appl. Phys. Lett.* 91, 111915 (2007). ISSN 00036951. http://link.aip.org/link/APPLAB/v91/i11/p111915/s1&Agg=doi.

96. D. Daniel, J. Walker, and J. Moore, 7, 53 (1998).

97. J.A. El-Awady, C. Woodward, D. Dimiduk, and N.M. Ghoniem, *Phys. Rev. B* 80, 1 (2009). ISSN 1098-0121. http://link.aps.org/doi/10.1103/PhysRevB.80.104104.

98. J. Fu , S.B. Joshi, and J.M. Catchmark, *J. Micromech. Microeng.* 18, 95010 (2008).

99. W. Moberly-Chan, D. Adams, M. Aziz, G. Hobler, and T. Schenkel, *MRS Bull.* 32 (2007).

100. S.J.A. Koh, H.P. Lee, C. Lu, and Q.H. Cheng, *Phys. Rev. B* 72, 085414 (2005).

101. M. Ke, S.A. Hackney, W.W. Milligan, and E.C. Aifantis, *Nanostruct. Mater.* 5, 689 (1995).

102. G. Wang, P. Liaw, Y. Yokoyama, A. Inoue, and C. Liu, *Mater. Sci. Eng. A* 494, 314 (2008). ISSN 09215093.

103. D. Farkas, S. Mohanty, J. Monk, *Mater. Sci. Eng. A* 493, 33 (2008), *Mechanical Behavior of Nanostructured Materials, a Symposium Held in Honor of Carl Koch at the TMS Annual Meeting 2007*, Orlando. .

104. J. Monk, and D. Farkas, *Phil. Mag.* 87, 2233 (2007).

105. H. Van Swygenhoven, and P.M. Derlet, *Phys. Rev. B* 64, 224105 (2001).

106. H. Van Swygenhoven, P. Derlet, and A. Hasnaoui, *Phys. Rev. B* 66, 024101 (2002).

107. V. Yamakov, D. Wolf, S.R. Phillpot, A.K. Mukherjee, and H. Gleiter, *Nat. Mater.* 1, 45 (2002).

108. W. Yin, S. Whang, and R. Mirshams, *Acta Mater.* 53, 383 (2005).

109. S. Frederiksen, K. Jacobsen, and J. Schiotz, *Acta Mater.* 52, 5019 (2004).

110. B. Yang, C. Motz, M. Rester, and G. Dehm, *Phil. Mag.* (2012). doi:DOI:10.1080/14786435.2012.693215.

111. P. Derlet, A. Hasnaoui, and H. Van Swygenhoven, *Scripta Mater.* 49, 629 (2003).

112. H. Van Swygenhoven, A. Caro, and D. Farkas, *Scripta Mater.* 44, 1513 (2001).

113. P. Derlet, and H. Van Swygenhoven, *Scripta Mater.* 47, 719 (2002).

114. H. Van Swygenhoven, P. Derlet, A. Hasnaoui, and M. Samaras, *Nanostructures: Synthesis, Functional Properties and Applications*, vol. 128, ed. T. Tsakalakos, I. Ovidko, A. Vasudevan (Kluwer Academic Publishers, Dordrecht, 2003) pp. 155–167.

115. V. Yamakov, D. Wolf, S. Phillpot, and H. Gleiter, *Acta Mater.* 51, 4135 (2003).

116. E. Rabkin, H.-S. Nam, and D. Srolovitz, *Acta Mater.* 55, 2085 (2007). ISSN 13596454. http://linkinghub.elsevier.com/retrieve/pii/S1359645406008202.

117. E. Rabkin, D.J. Srolovitz, *Nano Lett.* 7, 101 (2007). ISSN 1530-6984. http://www.ncbi.nlm.nih.gov/pubmed/17212447.

118. D. Mordehai, S.-W. Lee, B. Backes, D.J. Srolovitz, W.D. Nix, and E. Rabkin, *Acta Mater.* 59: 5202 (2011). ISSN 13596454. http://linkinghub.elsevier.com/retrieve/pii/S1359645411003132.

119. M. Horstemeyer, M. Baskes, and S. Plimpton. *Acta Mater.* 49, 4363 (2001).

120. H.S. Park, and J.A. Zimmerman, *Phys. Rev. B* 72, 054106 (2005).

121. G. Finbow, R. Lynden-Bell, and I. McDonald, *Mol. Phys.* 92, 705 (1997).

122. Z. Yang, Z. Lu , and Y.-P. Zhao, *Comput. Mater. Sci.* 46, 142 (2009).

123. N.S. Weingarten, and R.L.B. Selinger, *Modell. Simul. Mater. Sci. Eng.* 19, 015006 (2011).

124. B.E. Schuster, Q. Wei, H. Zhang, and K.T. Ramesh, *Appl. Phys. Lett.* 88, 103112 (2006). ISSN 00036951.

125. J.R. Trelewicz, and C.A. Schuh, *Acta Mater.* 55: 5948 (2007). ISSN 13596454. http://linkinghub.elsevier.com/retrieve/pii/S1359645407004685.

126. J. Trelewicz, and C. Schuh, *Phys. Rev. B* 79 (2009). ISSN 1098-0121. http://prb.aps.org/abstract/PRB/v79/i9/e094112.

127. N. Hansen, *Acta Metall.* 25, 863 (1977). ISSN 00016160. http://linkinghub.elsevier.com/retrieve/pii/0001616077901717.

128. R. Armstrong, *J. Mech. Phys. Solids* 9, 196 (1961).

129. J. Schiotz, K. Jacobsen. *Science* 301, 1357 (2003). http://www.sciencemag.org/cgi/content/abstract/301/5638/1357.

130. K. Kumar, S. Suresh, M. Chisholm, J. A. Horton, and P. Wang, *Acta Mater.* 51, 387 (2003). ISSN 13596454.

131. E. Bitzek, C. Brandl, P. M. Derlet, and H. Van Swygenhoven, *Phys. Rev. Lett.* 100, 1 (2008). ISSN 0031-9007. http://link.aps.org/doi/10.1103/PhysRevLett.100.235501.

132. D. Jia, K. Ramesh, and E. Ma, *Acta Mater.* 51, 3495 (2003). ISSN 13596454.

133. D. Huang, and P. Qiao, *J. Aerosp. Eng.* 24, 147 (2011).

134. K. Kumar, *Acta Mater.* 51, 5743 (2003). ISSN 13596454. http://linkinghub.elsevier.com/retrieve/pii/S1359645403005135.

135. D.S. Gianola, S. Van Petegem, M. Legros, S. Brandstetter, H. Van Swygenhoven, and K.J. Hemker, *Acta Mater.* 54, 2253 (2006).

136. R.J. Asaro, P. Krysl, B. Kad, *Philos. Mag. Lett.* 83, 733 (2003). ISSN 0950-0839. http://dx.doi.org/10.1080/09500830310001614540.

137. R.J. Asaro, and S. Suresh, *Acta Mater.* 53, 3369 (2005). ISSN 13596454.

138. P. Derlet, and H. Van Swygenhoven, *Phil. Mag. A* 82, 1 (2002). ISSN 0141-8610.

139. G. E. Dieter, *Mechanical Metallurgy*, 3rd ed. (McGraw-Hill, New York, 1986).

140. C. Can, Senior thesis at Caltech (2011).